Optimization of Rate Coefficients for Simplified Reaction Mechanisms with Genetic Algorithms

WOLFGANG POLIFKE,* WEIQUN GENG, and KLAUS DÖBBELING
ABB Corporate Research, CH-5405 Baden-Dättwil, Switzerland

A general procedure for determining optimum rate coefficients of simplified kinetic mechanisms is presented. The optimization's objective is to match heat release or net species production rates of the simplified and an underlying detailed kinetics mechanism. A genetic algorithm is employed to carry out the matching procedure with a minimum requirement of human effort and expertise. Applications of optimized two- and three-step schemes to lean-premixed laminar methane flames show very promising results: Profiles of temperature and main species and also the peak values of intermediate species match those obtained with the detailed kinetic mechanism very well; flame speeds have been reproduced with good accuracy. The optimized mechanisms have proven to be numerically robust and efficient; the flexibility and ease of use make the approach presented here particularly appropriate for the numerical modeling of combustion in situations of technical interest.

INTRODUCTION

The numerical simulation of turbulent reacting flows has made significant progress in recent years due to advances in physical modeling, development of detailed chemical mechanisms, computer hardware, and numerical algorithms. Nevertheless, the modeling of hydrocarbon combustion in situations of applied interest with a detailed chemical mechanism is out of reach for presently available tools, which accounts for the continued interest in methods for describing the chemical kinetics of hydrocarbon combustion more efficiently. The systematic reduction technique pioneered by Peters and co-workers (see [1–3] and references therein), the computational singular perturbation method (see, e.g., [4]), and the ILDM approach of Maas and Pope [5] are among the most prominent efforts in this area of research. However, the authors of the present paper are concerned with the modeling of lean-premixed combustion of natural gas in utility gas turbines, and they put forward that none of the available methods are well suited for this particular task.

The flows in gas turbine combustors are highly turbulent, and typical Reynolds, Damköhler, and Karlovitz numbers suggest that combustion model that rest on the "fast chemistry" assumption are not suited for the task at hand [6]. Instead, chemical time scales and the interaction of chemical kinetics with turbulence must be adequately accounted for. Promising candidates for this task are in our opinion (presumed) pdf models combined with reduced chemical kinetics. In order to keep the costs for large scale, three-dimensional computations within reasonable limits, the turbulent combustion model's chemical kinetics must be reduced to a system with at most two or three degrees of freedom. Algorithms that are computationally troublesome or expensive should be avoided whenever possible. The formulation of the chemistry model must not be restricted to constant equivalence ratio or constant total enthalpy.

Conflicting with this demand for efficiency, robustness, and universality is the fact that the gas turbine designer is interested in phenomena such as temperature distributions, lean blow-out limits, the effects of imperfect fuel-air premixing on the formation of oxides of nitrogen (NO_x), the influence of conductive or radiative heat losses or the admission of film cooling air on CO burn-out, etc. In order to model the influence of design changes on these phenomena, it is necessary to adequately describe mean heat release rates, finite rate chemistry effects (with sometimes widely different time scales!), concentrations of O-atom and other radicals, and formation and equilibration of CO, respectively.

An approach that in our opinion represents an acceptable compromise between these conflicting requirements is the use of simplified two- or at most three-step mechanisms with rate expressions in generalized (i.e., with non-integer species concentrations exponents) Arrhe-

*Corresponding author.

COMBUSTION AND FLAME 113:119–135 (1998)

Published by Elsevier Science Inc.
0010-2180/98/$19.00
PII S0010-2180(97)00212-5

nius form. Such a formulation is very efficient, robust, and easy to implement. The problem is then, of course, the selection of the simplified reactions and in particular the choice of reaction rate coefficients. This is where the present work attempts to make a contribution. Rather than trying to determine rate expressions by fitting to global properties of reacting flows, e.g., laminar flame speed, in our approach the rate coefficients of the simplified mechanism are adjusted to reproduce heat release and net species production rates obtained with an underlying detailed mechanism (henceforth called the "base mechanism"). This strategy has been suggested earlier by Nastoll [7] and is reminiscent of the work of Coffee et al. [8], who determined rate coefficients of single-step global mechanisms by fitting to (experimentally) observed heat release profiles of laminar flames. Only recently has the work by Jiang et al. [9] and Nicol [10] come to our attention, where an approach similar to ours is described, albeit in the context of reactive blast wave flows and chemical reactors, respectively. The use of a genetic algorithm for the matching of production rates distinguishes our approach.

It should be emphasized that our goal is not to find one set of rate coefficients that is valid for a wide range of conditions. Instead, it has been attempted to develop a method which allows to extract quickly and without detailed investigation of the chemical kinetics rate coefficients for a simplified mechanism from a given set of (detailed) chemical data. Nevertheless, as we are using Arrhenius rate expressions, we expect (and this expectation has been confirmed; see below) that any given set of rate coefficients may be used for a certain range of operating conditions, e.g., equivalence ratio, inlet temperature, or (total) enthalpies, with reasonable accuracy. This is particularly useful for the treatment of slight inhomogeneities of fuel-air premixing, cooling air admission, or non-adiabatic effects.

We concede that the restriction of any set of rate coefficients derived with our method to a narrow range of conditions is an undesirable limitation. However, in practice this is often outweighed by the computational efficiency of our formulation.

The paper is organized as follows: In the next section, some of the more well-known methods for simplifying chemical kinetics and their applicability to modeling combustion in gas turbines are reviewed briefly. As a preliminary to the presentation of rate coefficient optimization algorithms and results, the difficulties of representing consistently rate data from detailed chemical mechanisms by simplified mechanisms with their limited number of degrees of freedom are discussed. Consequences resulting from a "representability analysis" for the related problem of finding reaction rate coefficients for rate laws in Arrhenius form are presented. Then the basic idea of a genetic algorithm is outlined, supplemented by application-specific details of implementation. The subsequent sections present the results of rate coefficient optimization for two- and three-step mechanisms for methane at atmospheric and elevated pressures. A validation of optimized rate coefficients is carried out by comparing freely propagating laminar flame computations with simplified and detailed mechanisms, respectively. Extensions to strained laminar flames and other "off-design" applications complete the presentation of results achieved so far. In the Conclusions, the potential and limitations of our approach are summarized.

REVIEW OF ALTERNATIVE APPROACHES

The efforts in developing global reaction schemes for hydrocarbons date back to the late 1950's; see, e.g., the review by Abdalla et al. [11]. The earlier works were based on experimental data obtained with well-stirred and turbulent flow reactors. Unfortunately, the global rate expressions obtained with this approach are of very limited accuracy, presumably due to the limitations inherent in using a single-step mechanism and the effect of interactions between chemistry and mixing processes.

Using a numerical model for a one-dimensional freely propagating laminar flame, Westbrook and Dryer [12] determined rate expressions for one- and two-step hydrocarbon oxidation schemes by fitting to experimentally observed laminar flame speeds. With non-unity reaction orders for both fuel and oxidizer, the reaction schemes of Westbrook and Dryer produced flame speeds that match experimental

values quite well over a wide range of equivalence ratios and pressures. See, however, the discussion of transport coefficients and numerical subtleties due to negative species concentration exponents in Coffee's contribution [13]. Also, none of the simplified mechanisms studied accurately describes the chemical structure of the flame, and the treatment of CO equilibration is not suitable for our purposes.

To investigate in detail the reaction paths and time scales of a chemical mechanism, and to utilize the knowledge thereby obtained in the construction of a reduced mechanism, is the concept behind the so-called *systematic reduction* of kinetic mechanisms of Peters and coworkers [1–3]. A major difficulty of this approach is that the rate expressions resulting from the reduction procedure may be algebraically complicated and can pose severe numerical difficulties. The so-called truncation of rate expressions alleviates this problem; however, it invokes additional steady-state assumptions, whose validity is not always assured. Also, considerable expertise and effort are required to construct a reduced mechanism. For premixed methane-air flames, a reduced four-step mechanism [3] with seven species (plus inert nitrogen) yields very good agreement with the underlying detailed mechanism over a wide range of operating conditions. Unfortunately, the four-step mechanism for methane is already too complex and computationally expensive for the applications envisaged here. Further reducing the mechanism invokes steady-state or partial equilibrium assumptions that are not well justified at the low temperatures ($T \approx 1800$ K) typical of lean-premixed gas turbine combustion [14].

Jones and Lindstedt [15] use a systematically reduced four-step mechanism as a starting point for further simplifications, eliminating radical species and constructing algebraically simple and numerically robust rate expressions. Unfortunately, the reaction rate coefficients given in [15] are reported to yield only poor agreement with detailed kinetics at lean conditions [11].

Similar to systematic reduction, the method of computational singular perturbation (CSP) identifies fast time scales and eliminates the corresponding quasi-steady-state species to arrive at a reduced mechanism. The time scale analysis is done automatically (based on the local Jacobian) and dynamically, i.e., both the number and the identity of the slow species that the reduced mechanism comprises may change as the reactions progress. Owing to the high computational cost of this analysis [16], CSP is not suited for our purposes.

The ILDM method introduced by Maas and Pope [6] also exploits the local Jacobian for the elimination of fast time scales: those eigenvectors of the Jacobian that correspond to slowest time scales are used to construct an intrinsic lower dimensional manifold, on which a (small) number of slow parameterizing variables evolve. It is argued that the fast variables always drive the system quickly towards the ILDM; therefore the dynamics of the parameterizing variables within the slow manifold provides a good approximation to the behavior of the complete system. In applications of the ILDM method to combustion modeling, a preprocessing step is required, where the dynamics of the slow variables in relevant regions of phase space is stored in lookup-tables. The lookup-table approach is obviously advantageous inasmuch as it avoids algebraically complicated rate expressions and reduces computational cost. However, for systems of applied interest, this approach might prove to be a serious disadvantage: the effects of non-adiabaticity and imperfect fuel-air mixing require an extension of the table by two dimensions, which might make the generation and storage of the tables as well as the lookup-procedure prohibitively expensive. Also, it seems that the implementation of the ILDM method is not an easy task, and only recently have applications to methane be reported [17].

GOVERNING EQUATIONS FOR PREMIXED LAMINAR FLAMES

As mentioned in the Introduction, rate data from laminar flame computations are used to generate and validate optimized reaction rate coefficients for simplified mechanisms. In this section, we summarize briefly the equations required for the formulation of the premixed flame model with a detailed or simplified chemical mechanism. For more details, the reader is referred to references [2, 18, 21].

A chemical mechanism with N species and L

reactions may be represented in the following form:

$$\sum_{n=1}^{N} \nu'_{nl} C_n \leftrightarrow \sum_{n=1}^{N} \nu''_{nl} C_n;\ l = 1, \ldots, L, \tag{1}$$

where $C_n (n = 1, \ldots, N)$ is the chemical symbol of the nth species, and ν'_{nl}, ν''_{nl} are the forward and backward stoichiometric coefficients of the nth species in the lth reaction, respectively.

The reaction rates $\mathbf{r} = \{r_l;\ l = 1, \ldots, L\}$ determine the molar rate of production of species C_n, denoted $\dot{\omega}_n$, and the rate of heat release per unit volume $\dot{q}$:

$$\dot{\omega}_n = \sum_{l=1}^{L} \nu_{nl} r_l, \tag{2}$$

$$\dot{q} = -\sum_{l=1}^{L} h_l r_l, \tag{3}$$

where $\nu_{nl} = \nu''_{nl} - \nu'_{nl}$, while h_l (which is the change in enthalpy associated with passing completely from reactants to products in the lth reaction) is obtained as an appropriately weighted sum over the standard state enthalpies H_n (in molar units) of those species that participate in the reaction:

$$h_l = \sum_{n=1}^{N} \nu_{nl} H_n. \tag{4}$$

Note that using Eq. (2), expression (3) for the rate of heat release can easily be put in the more familiar form $\dot{q} = -\Sigma_{n=1}^{N} \dot{\omega}_n H_n$.

For both the detailed and global mechanisms considered in this paper, a *rate law* of the following form determines the reaction rates $\mathbf{r}$ in dependence of molar species concentrations $[C_n]$ and rate constants k:

$$r_l = k_{fl} \prod_{n=1}^{N} [C_n]^{\tilde{\nu}'_{nl}} - k_{rl} \prod_{n=1}^{N} [C_n]^{\tilde{\nu}''_{nl}};\quad l = 1, \ldots, L, \tag{5}$$

where an Arrhenius temperature dependence for the rate constants k_{fl} (forward) and k_{rl} (reverse) is assumed:

$$k_l = A T^n \exp\left(-\frac{E_A}{RT}\right). \tag{6}$$

Note that for a detailed mechanism composed of elementary reactions, the species concentration exponents $\tilde{\nu}_{nl}$ appearing in the rate law (5) are equal to the stoichiometric coefficients ν_{nl} of the mechanism (1). For a simplified mechanism, this is in general not the case.

The production rates of species $\dot{\omega}_n$ and heat $\dot{q}$ appear as source terms in the equations for mass fractions Y_n and temperature T describing a steady, one-dimensional isobaric flame

$$\dot{m} \frac{\mathrm{d}Y_n}{\mathrm{d}x} + \frac{\mathrm{d}}{\mathrm{d}x}(\rho Y_n V_n) = \dot{\omega}_n W_n,\ n = 1, \ldots, N, \tag{7}$$

$$c_p \dot{m} \frac{\mathrm{d}T}{\mathrm{d}x} - \frac{\mathrm{d}}{\mathrm{d}x}\left(\lambda \frac{\mathrm{d}T}{\mathrm{d}x}\right) + \sum_{n=1}^{N} \rho Y_n V_n c_{pn} \frac{\mathrm{d}T}{\mathrm{d}x} = \dot{q}. \tag{8}$$

In these equations, $\dot{m} = \rho u$ denotes an overall mass flow rate per unit area, which is constant throughout the flame; V_n the diffusion velocity and W_n the molecular weight of the nth species; ρ the density; c_p and c_{pn} the heat capacity at constant pressure of the mixture and the nth species, respectively, and λ the mixture thermal conductivity. The ideal-gas equation of state $\rho = p\bar{W}/RT$ is invoked to close the system of equations.

Equations (7) and (8) describe an unstrained, freely propagation flame. Note that in this case, the mass flow rate $\dot{m}$ is not freely prescribed but instead obtained as part of the solution and determines the laminar flame speed $S_L = \dot{m}/\rho_c$, where the subscript c refers to the cold state. For further details, e.g., details on the transport model used to compute the diffusion velocities V_n or the governing equations for the strained laminar premixed flame model, the interested reader is requested to consult [3, 18].

The laminar flame model has been computed with the RUN1DL program provided by Rogg [3, 18, 19]; the base mechanism used throughout this paper is that of Miller and Bowman [20] with 52 species and 268 reactions. For post-processing, i.e., determination of heat release and production rates, the CHEMKIN package [21] has been used.

REPRESENTABILITY OF REACTION RATE DISTRIBUTIONS

A reduced or "simplified" mechanism has obviously fewer degrees of freedom, i.e., species and reactions, than a detailed mechanism. This poses of course the question to what extent the heat release and species production rates obtained with a detailed mechanism can be represented *consistently* by a simplified mechanism.

Equations (2) and (3) for the molar rates of species production $\dot{\omega}_n$ and the rate of heat release $\dot{q}$ establish a linear set of relations between the reaction rates $\mathbf{r} = \{r_l;\ l = 1, \ldots, L\}$ and a production rate vector ***p:***

$$\boldsymbol{p} \equiv \{\dot{\omega}_1; \ldots \dot{\omega}_N; \dot{q}\}, \tag{9}$$

which may be written in the following form

$$\boldsymbol{p} = \mathcal{M}\mathbf{r}. \tag{10}$$

The coefficients of the $L \times N$ matrix $\mathcal{M}$ are easily determined from Eqs. (2) and (3).

A chemical mechanism has usually more reactions than species; the matrix $\mathcal{M}$ is not quadratic and has no inverse. It follows that given an arbitrary set of production rates $\boldsymbol{p}$, it is in general *not* possible to find a set of reaction rates $\mathbf{r}$ which fulfills Eq. (10). This could obviously jeopardize our approach, as we are trying to find a set of reaction rates for a simplified mechanism $\{r_l;\ l = 1, \ldots, L_S\}$ that reproduces production rates $\{p_n;\ n = 1, \ldots, (N_S + 1)\}$ observed with the base mechanism (Here the subscript S refers to the simplified mechanism). As a simple example, consider the fuel breakdown reactions in a detailed mechanism, which consume fuel without releasing much heat and thereby decouple to some extent fuel consumption and heat release rates. Clearly, this behavior cannot be reproduced with, e.g., a simple one-step mechanism, where species production and heat release rates are all proportional to each other. Similar constraints are also imposed in two- or three-step mechanisms by element conservation, etc. It is important to understand that this issue of "representability" is not related to the problem of determining the rate law, i.e., the functional dependence of reaction rates on species concentrations and temperature. Indeed, all (systematically) reduced or simplified mechanism are confronted with this problem, and the question is not whether a simplified mechanism can represent its base mechanism consistently (it usually cannot) but whether the unavoidable inconsistencies and discrepancies are within acceptable limits.

In order to verify that a given set of production rates provided by the base mechanism can be represented with reasonable consistency within the framework of a simplified mechanism, we proceed as follows. From the simplified mechanism's set of production rates, a subset of rates $\{\tilde{p}_n;\ n = 1, \ldots, L_S\}$ is selected, resulting in a reduced system of equations:

$$\tilde{\mathbf{p}} = \tilde{\mathcal{M}}\tilde{\mathbf{r}}, \tag{11}$$

In this paper, we refer to the selected subset of rates $\tilde{\mathbf{p}}$ and the corresponding species as *principal rates* and *principal species*, respectively. Guidelines for selecting the principal rates from the complete set of production rates will become apparent in the remainder of the paper. The rates $\{p_n;\ n = L_S + 1, \ldots, N_S\}$ are called the *minor rates* and correspondingly *minor species*. Note that educts, products and intermediates may be principal as well as minor species.

The $L_S \times L_S$ matrix $\tilde{\mathcal{M}}$ is obtained by eliminating rows that correspond to minor production rates from $\mathcal{M}$. If the principal rates $\tilde{\mathbf{p}}$ are linearly independent, $\tilde{\mathcal{M}}$ is invertible, and reaction rates $\tilde{\mathbf{r}}$ can now be determined from the principal rates

$$\tilde{\mathbf{r}} = \tilde{\mathcal{M}}^{-1}\tilde{\mathbf{p}}. \tag{12}$$

Now the minor production rates corresponding to the set of reaction rates $\tilde{\mathbf{r}}$ can be computed with the help of (10) and compared with the minor production rates as they are provided by the global mechanism. If the agreement is reasonable, one may conclude that the simplified mechanism is capable of representing the production rate distributions of the base mechanism with a fair degree of consistency.

This is best illustrated with an example. Consider a simplified 2-step mechanism for methane with CO as an intermediate:

$$\begin{aligned} 2CH_4 + 3O_2 &\rightarrow 2CO + 4H_2O, \\ 2CO + O_2 &\rightarrow 2CO_2. \end{aligned} \tag{13}$$

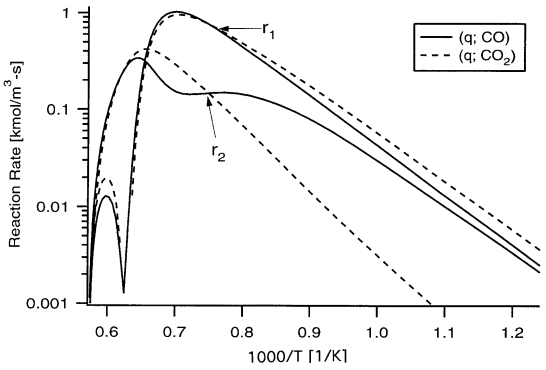

Fig. 1. Two-step mechanism (13): Reaction rates $\tilde{r}_1$ and $\tilde{r}_2$ vs inverse temperature. Continuous lines: principal rates ($\dot{q}$; $\dot{\omega}_{CO}$), dashed lines: principal rates ($\dot{q}$; $\dot{\omega}_{CO_2}$). Rate data are taken from a computation of a freely propagating laminar flame with the base mechanism.

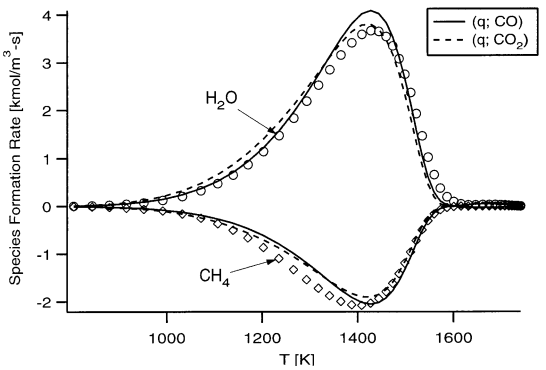

Fig. 2. Two-step mechanism (13): Comparison of minor formation rates from the detailed mechanism (Markers ○ and ◇ for H_2O and CH_4, respectively) with rates computed from $\tilde{r}_1$ displayed in Fig. 1. Continuous lines: principal rates ($\dot{q}$; $\dot{\omega}_{CO}$), dashed lines: principal rates ($\dot{q}$; $\dot{\omega}_{CO_2}$).

With this mechanism, any combination of species production or heat release rates may be used as principal rates. However, as the rate of heat release is of prime importance for temperature distribution and flame propagation, it seems natural to select $\dot{q}$ as one of the principal rates. Another quantity of interest is carbon monoxide concentration, so one may select $\dot{\omega}_{CO}$ as the second principal rate. In this case,

$$\tilde{\mathcal{M}} = \begin{pmatrix} -h_1 & -h_2 \\ 2 & -2 \end{pmatrix}. \tag{14}$$

The inverse matrix $\tilde{\mathcal{M}}^{-1}$ is easily determined, and one obtains

$$\begin{pmatrix} \tilde{r}_1 \\ \tilde{r}_2 \end{pmatrix} = \frac{1}{h_1 + h_2} \begin{pmatrix} -1 & h_2/2 \\ -1 & -h_1/2 \end{pmatrix} \begin{pmatrix} \dot{q} \\ \dot{\omega}_{CO} \end{pmatrix}. \tag{15}$$

The reaction rates $\tilde{\mathbf{r}}$ of the two-step mechanism (13) obtained with this procedure from the heat release and CO production rates found in a freely propagating laminar flame at operating pressure $p = 1$ bar, equivalence ratio $\phi = 0.5$ and inlet temperature $T_o = 630$ K are shown in Fig. 1 for temperatures T ranging from inlet temperature to adiabatic flame temperature.

Also shown in the Figure are reaction rates $\tilde{\mathbf{r}}$ with $\dot{q}$ and $\dot{\omega}_{CO_2}$ selected as principal rates. The graph shows that for the first reaction it does not matter much whether $\dot{q}$ and $[\dot{CO}]$ or $\dot{q}$ and $[\dot{CO}_2]$ are used as principal rates. However, the rate $\tilde{r}_2$ of the CO oxidation reaction does depend significantly on the choice of principal rates.

The production rates of minor species, i.e., CH_4, H_2O, and CO or CO_2, respectively, obtained from these reaction rates are compared against those of the detailed mechanism in Figs. 2 and 3, again for both combinations of principal rates. For both methane and water, the overall agreement is satisfactory. One can observe that in the detailed mechanism, CH_4 consumption rates are slightly higher at lower temperatures. As already discussed above, this is due to the detailed mechanism's fuel breakdown reactions, which consume CH_4 without releasing significant amounts of heat. In the simplified mechanism, these intermediate reactions are absent, and CH_4 consumption is nec-

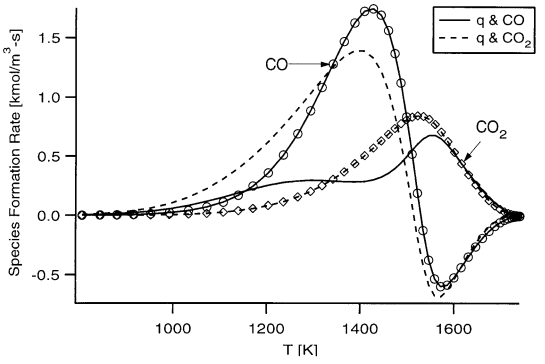

Fig. 3. Two-step mechanism: Comparison of formation rates of CO and CO_2 from the detailed mechanism (Markers) and computed from $\tilde{r}_1$ and $\tilde{r}_2$ displayed in Fig. 1. Continuous lines: ($\dot{q}$; $\dot{\omega}_{CO}$) as principal rates. Dashed lines: ($\dot{q}$; $\dot{\omega}_{CO_2}$) as principal rates.

essarily linked to heat release and production of CO and H_2O.

The production rates of CO_2 and CO computed from $\tilde{\mathbf{r}}$ and Eq. (10), on the other hand, are influenced strongly by the choice of principal rates; see Fig. 3. Specifically, if CO_2 is one of the principal rates, CO production in the simplified mechanism appears shifted towards lower temperatures and peaks at a lower value than in the detailed mechanism, and similarly for CO_2 production if CO is the second principal rates.

Note that up to this point, no assumptions whatsoever have been made concerning the rate law, i.e., the dependence of reaction rates $\tilde{\mathbf{r}}$ on species concentrations and temperature. If we assume that a rate law of the form (5) with an Arrhenius temperature dependence for the rate constants k also holds for the simplified mechanism, and we have argued in the Introduction that this is advantageous to our purposes, we must obviously also examine whether the rates $\tilde{\mathbf{r}}$ are consistent with this ansatz. In this respect, examination of Fig. 1 reveals some discrepancies: the non-monotonous behavior of $\tilde{r}_1$ with the kink near 0.625 1000/K is clearly incompatible with the assumed form of the rate law. Note, however, the logarithmic scale of the ordinate in Fig. 1; the overall error made in not being able to represent the kink in reaction rate is of the order of 1%. Similarly, the behavior of $\tilde{r}_2$ with $(\dot{q};\ \dot{\omega}_{CO})$ as principal rates seems incompatible with our rate law ansatz, although this cannot be said with certainty as long as the exponent for CO concentration in the rate law for r_2 is not determined. From this observation one may infer that CO_2 is to be preferred as the second principal rate.

One may conclude for this example that the simple two-step mechanism (13) with a rate law in generalized Arrhenius form and $(\dot{q},\ \dot{\omega}_{CO_2})$ as principal rates is fairly consistent with the heat release and species production distributions observed in a numerical simulation of a freely propagating flame with a detailed chemical mechanism. Discrepancies are observed with respect to the fuel consumption reaction at high temperatures, and with respect to CO-oxidation at intermediate temperatures. Our experience with the optimized two-step scheme does indicate, however, that the impact of these discrepancies on flame speed and carbon monoxide concentrations in a flame simulation with the two-step mechanism is tolerable (see the following section). Note that at other operating conditions or with other reaction schemes, the representibility of the base mechanism's rates by the simplified mechanism has been observed to be qualitatively different from what has been observed here. It is therefore recommended to evaluate various selections of principal rates and the resulting reaction rates and minor rates for every operating condition anew.

OPTIMIZATION OF RATE COEFFICIENTS WITH GENETIC ALGORITHMS

"Genetic algorithms," also known as "evolution strategies" [22], are optimization algorithms that imitate principles of biological evolution. The development of these methods has been driven by the premise that genetic algorithms should be particularly powerful and efficient optimization strategies because biological evolution has not only optimized its products, but also its *methods*. Key ingredients of typical genetic algorithms (GA) are a "population" of "individuals," each described or parameterized by a set of "genes." The "individuals" undergo a process of "selection," such that only the "fittest" individuals of every "generation" survive to beget the next generation. In the process of generating the next generation's individuals from the parents' "gene pool," genetic information is exchanged among the parents ("recombination") and some random "mutations" occur.[1]

Genetic algorithms have been successfully applied to nonlinear optimization problems in many dimensions, where more traditional methods can fail because an initial guess that lies within the radius of convergence of the method is difficult to find. Also, deterministic, gradient-based optimization methods tend to "get stuck" in local extrema of the fitness function (some-

[1] When transferring the concepts of evolution to a technical or numerical optimization problem, the biological terms could of course be translated into technical language, e.g., "populations" would be "ensembles," "chromosomes" would be "system parameters," etc. However, the technical terms do not carry the connotations of their biological counterparts, which is why we feel that these concepts are best explained using the language of biology.

times referred to as the cost function) and are therefore ill suited for problems where the fitness varies non-monotonously with the parameters. GAs, on the other hand, are able to depart from local extrema due to the variability of parameters within the "gene pool" and the element of randomness inherent in the methods. Third, GAs do not require knowledge of the gradient of the fitness functions, which makes them particularly suited for optimization problems where an analytical expression for the fitness function is not known.

In applications to the present optimization problem, we have noticed another beneficial quality of GAs: If the algorithm's progress strategy is oriented more towards recombination of genetic information within the population rather than random mutation, then the chromosomes usually do not stray far outside the region of parameter space that was populated by the first generation. It is therefore very easy to avoid parameter values that seem physically unreasonable (e.g., negative or extremely large activation energies) or numerically undesirable (e.g., negative species concentration exponents) by simply initializing the optimization process appropriately. Traditional linear or non-linear[2] optimization routines [23] do in our experience often result in unreasonable parameter values—even if they are started from a converged GA search, and in particular so for linear methods.

When applying genetic algorithms to a technical or numerical optimization problem, the details of implementation will depend strongly on the problem at hand. We have used a variant of the so-called $(\mu + \lambda)$ algorithm developed by Rechenberg and co-workers [22]. In this scheme, a population evolves through a sequence of generations. The population consists of μ parents, each of which is uniquely characterized by a certain number of parameters (chromosomes). The fitness must be a continuous function of the chromosomes. Per generation a certain number λ of children are created by selecting chromosomes at random from the parent population's gene pool. In addition, the chromosomes of the children also undergo random mutations. From the total population of $\mu + \lambda$ individuals, the μ fittest ones are selected to constitute the next generation.

The algorithm, although conceptually quite complex, can be programmed rather elegantly and compactly, a detailed description and a discussion of its variants are given in the monograph by Rechenberg [22].

Turning now to details of our application, we first outline again our strategy: Gas turbine (or test stand) operating conditions determine pressure p, inlet temperature T_o, and equivalence ratio ϕ at which combustion takes place. In order to optimize the rate coefficients of a given simplified mechanism for one such set of conditions, it is necessary to obtain first a sufficiently large set of characteristic temperatures, species concentrations, and production rates. This may be done, for example, by computing a one-dimensional freely propagating laminar flame at the chosen values of p, T_o, and ϕ. This will produce a set of temperatures $T(i)$ and species concentrations $[C_n](i)$, related heat release rates $\dot{q}(i)$ and species production rates $\dot{\omega}_{C_n}(i)$, where the i's enumerate the grid points of the laminar flame computation and $n = 1, \ldots N_D$, with N_D being the number of chemical species of the detailed mechanism. Once a set of principal rates $\{\tilde{p}_n;\ n = 1, \ldots, L_S\}$ has been determined (see the previous section), the GA is employed to find a set of rate coefficients that yields a good match between the reaction rates $\mathbf{r}(i)$ of the simplified mechanism and the reaction rates $\tilde{\mathbf{r}}(i)$ determined from the base mechanism's principal rates. If a good match between $\mathbf{r}(i)$ and $\tilde{\mathbf{r}}(i)$ can be found—which requires that the dependence of the $\tilde{\mathbf{r}}(i)$ on temperature and species concentrations is not incompatible with the Arrhenius ansatz, and if the selected principal rates allow a consistent representation of detailed rate data with the simplified mechanism, then heat release rates and net production rates of all the species of the simplified mechanism will match those of the detailed mechanism.

One of the crucial points in adopting the $(\mu + \lambda)$ strategy to the present task is the

[2] Note that at least for the special case of a single-step mechanism without reverse reactions one may easily reduce the problem of finding optimal Arrhenius coefficients to a linear one by taking the logarithm of the rate law (5). Then standard techniques like the linear least squares method may be applied.

definition of the fitness function, which the evolution strategy needs for the selection step. It must be a suitably defined measure of the closeness with which the rates of the global mechanism match those of the base mechanism. The problem is not trivial because production rates vary by several orders of magnitude and a matching criterion that concentrates only on peak values will not be able to distinguish between a good and a bad fit. The standard root mean square (rms) deviation is therefore usually not appropriate here. Instead, the following criterion, which in some sense considers deviations on a logarithmic scale, has been used:

$$f_l = \left\langle \left| \ln \left(\left| \frac{r_l(i)}{\tilde{r}_l(i)} \right| \right) \right| \left| \frac{\tilde{r}_l(i)}{\max\,(\tilde{r}_l)} \right|^{\eta} \right\rangle. \qquad (16)$$

Here $r_l(i)$ denotes the lth reaction rate of the simplified mechanism with the generalized Arrhenius rate law, while the $\tilde{r}$ refers to the detailed mechanism. The determination of the maximum $\max(\tilde{r}_l)$ and the average $<\cdots>$ is carried out over all grid points x_i, $i = 1, \ldots N_{\text{grid}}$. Obviously, the logarithm of the ratio of reaction rates is just the deviation on a logarithmic scale, while the second factor (with $\eta = 0.2 - 0.5$) allows to adjust the weight of very small rates on the overall fitness criterion.[3]

At this point, another advantage of the representability analysis based on principal rates becomes apparent. If one was to try to directly match, for example, heat release and CO_2 production rates for a two-step mechanism like (13), it would be necessary to optimize the rate coefficients of both reactions simultaneously and to define a fitness function that provides a measure of "overall fitness" for both $\dot{q}$ and $\dot{\omega}_{CO_2}$. With the approach suggested by the representability analysis, it is always possible to employ a *divide and conquer* strategy and optimize the rate coefficients of only one reaction at a time.

TWO-STEP MECHANISM

In a prior section, we carried out the representability analysis for the simple two-step mechanism (13), using data from a freely propagating premixed laminar flame computation at operating pressure $p = 1$ bar, inlet temperature $T_0 = 630$ K, and equivalence ratio $\phi = 0.5$. This set of data shall also serve as a first test case for the rate coefficient optimization. The success of the optimization can be judged directly by comparing the principal rates $\tilde{\mathbf{r}}$ of the base mechanism against the rates $\mathbf{r}$ of the optimized mechanism, or indirectly by comparing, e.g., flame speeds and temperature or species mass fraction profiles produced by laminar flame computations with the base and the simplified mechanism, respectively.

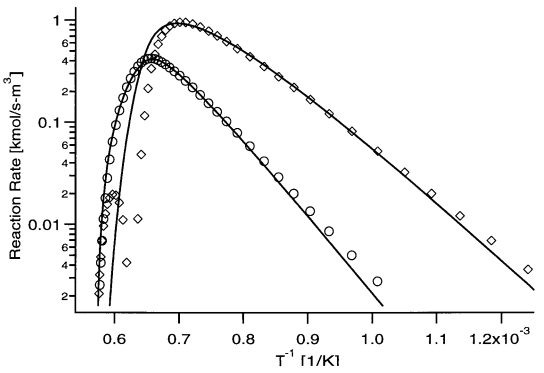

Fig. 4. Comparison of optimized rates (—) for the two-step mechanism (13) with rate coefficients 2/qc2/p1 (see Table 1) and principal rates $\dot{q}$ (◇) and $\dot{\omega}_{CO_2}$ (○) of the base mechanism (detailed concentration and rate data taken from a freely propagating flame computation at $p = 1$ bar, $T_o = 630$ K, and $\phi = 0.5$).

Choosing a population size $\mu = 24$ with $\lambda = 64$ children per generation, the genetic algorithm typically ceases to make progress after several hundred generations, consuming a few minutes of *CPU* time on a modern desktop computer. Note that for a given set of (detailed) chemical kinetic data, the genetic algorithm does not produce a unique result. Different starting conditions or parameter settings do yield different solutions, i.e., values for the rate coefficients, although in general with comparable fitness, suggesting either that the optimization problem is underdetermined, or that the algorithm cannot find a *global* optimum.

If heat release rate $\dot{q}$ and $\dot{\omega}_{CO_2}$ are used as principal rates, the achieved match between the principal rates $\tilde{\mathbf{r}}$ of the base mechanism and the rates $\mathbf{r}$ of the optimized mechanism is quite

[3] Note that a good match will produce a small value of f_l, so the goal of the optimization strategy is actually to minimize rather than maximize the fitness function, which in this case is often termed the "cost function."

TABLE 1

Reaction Rate Coefficients for Optimized Two- and Three-step Mechanisms. $\phi = 0.5$, $T_i = 630$ K, $p = 1$ bar.

		Species Concentration Exponents $\tilde{\nu}_{nl}$							
Name	Principal Rates	CH_4	O_2	CO	H_2O	H_2	$\log_{10}(A)$	n	E_A/R
2/qc2/p1	q, CO_2	0.4439	0.9228	0	0	—	9.250	0	14941
		0	0.6029	1.4512	0	—	11.408	0	15497
2/qc/p1	q, CO	0.4439	0.9228	0	0	—	9.250	0	14941
		0	1.0363	1.2386	0	—	10.917	0	11980
3/fw2/p1	CH_4, H_2O, CO_2	0.629	0.3151	0	0	0	8.423	0	14326
		0	0	1.2381	0.6519	0	10.238	0	12467
		0	0.2601	0	0	2.0099	11.859	0.9595	15937
3/qh2/p1	Q, H_2, CO_2	0.4453	0.4314	0	0	0	8.026	0	14350
		0	0	1.0006	0.7332	0	9.555	0	12308
		0	0.138	0	0	1.7597	12.248	0	12293

good, with the exception of the local minimum near $T = 1600$ K of the first reaction; see Fig. 4. Note that the rate coefficients of this and all other optimized mechanism discussed in this paper are summarized in Tables 1 and 2. Combined with the equations summarized in a prior section, it should be clear how production rates for the simplified mechanism are determined from the rate coefficients listed in the tables. However, if the production rate of CO is selected as the second principal rate, the optimization is not able to find a match of similar quality for the second reaction; see Fig. 5. These findings are in accordance with the remarks made above that one is advised to choose principal rates that yield rate laws compatible with the Arrhenius ansatz.

The direct comparison of production rates suggests that the optimized two-step mechanism should be capable of reproducing propagation speed and structure of the laminar flame computation with the base mechanism fairly well. Figures 6 and 7 show that this is indeed so, with the exception of the temperature rise in the flame's reaction zone and CO burn-out, which are both overpredicted by the simplified mechanism. The laminar flame speed obtained with the two-step mechanisms is $s_L = 0.525$ m/s (with $\tilde{\mathbf{p}} = \{\dot{q}, \dot{\omega}_{CO_2}\}$), and $s_L = 0.533$ m/s (with $\tilde{\mathbf{p}} = \{\dot{q}, \dot{\omega}_{CO}\}$), which compares reasonably well

TABLE 2

Reaction Rate Coefficients for Optimized Two- and Three-step Mechanisms. $\phi = 0.5$, $T_i = 753$ K, $p = 20$ bar.

		Species Concentration Exponents $\tilde{\nu}_{nl}$							
Name	Principal Rates	CH_4	O_2	CO	H_2O	H_2	$\log_{10}(A)$	n	E_A/R
2/qc2/p20	q, CO_2	0.5458	0.2488	0	0	—	10.540	—	24044
		0	0.8374	1.7902	0	—	14.193	0.4730	30145
2/hc2/p20	H_2O, CO_2	0.5482	0.1194	0	0	—	10.099	—	23182
		0	0.7745	1.6132	0	—	13.180	0.5117	29065
3/fw2/p20	CH_4, H_2O, CO_2	0.6677	0.5875	0	0	0	11.824	—	23800
		0	0	1.0574	0.7745	0	11.769	—	21575
		0	0.3331	0	0	1.1295	13.089	—	23238
3/qh2/p20	Q, H_2, CO_2	0.5898	0.1887	0	0	0	10.091	0.2376	23786
		0	0	1.0525	0.6957	0	9.629	0.4585	19633
		0	0.597	0	0	1.314	11.021	1.0117	23263

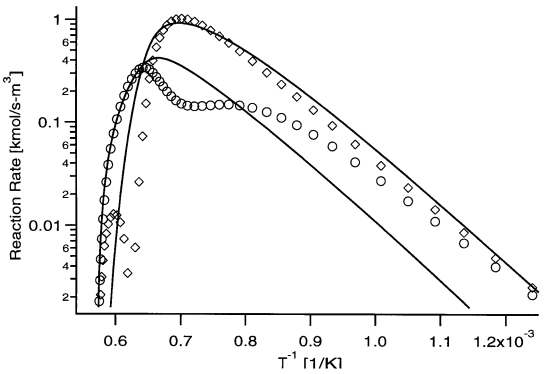

Fig. 5. Comparison of optimized rates (—) for the two-step mechanism (13) with rate coefficients 2/qc/p1 and principal rates $\dot{q}$ ($\diamond$) and $\dot{\omega}_{CO}$ ($\bigcirc$) (*cf*. Fig. 4).

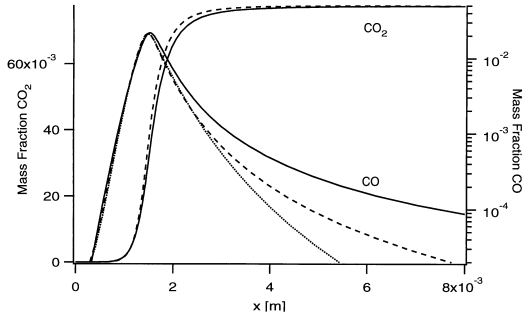

Fig. 7. CO_2 and CO profiles of laminar flames computed with the base (—) and optimized two-step mechanism with rate coefficients 2/qc2/p1 (– – –) and 2/qc/p1 ($\cdots$) as principal rates. At equilibrium, mass fraction of CO $\approx 1.7 \times 10^{-5}$. Note that the x-axis scale is not the same as in Fig. 6.

with the value $s_L = 0.482$ m/s obtained with the detailed mechanism. Somewhat surprisingly, as far as temperature and main species are concerned, it does not make a significant difference whether $\{q,\ \dot{\omega}_{CO_2}\}$ or $\dot{q},\ \dot{\omega}_{CO}\}$ are used as principal rates: profiles of the said variables obtained with the two different sets of rate coefficients are indistinguishable from each other on plots like Fig. 6 (not shown). In this instance, poor representability did result in discrepancies when comparing optimized and principal rates directly (see the beginning of this section) but did not adversely affect the performance of the simplified mechanism in the validation computation.

The overpredicted temperature at the end of the fuel consumption region is in our opinion due to the absence of radicals or intermediates other than CO and could be responsible for accelerated CO burn-out as well as the overpredicted laminar flame speed.

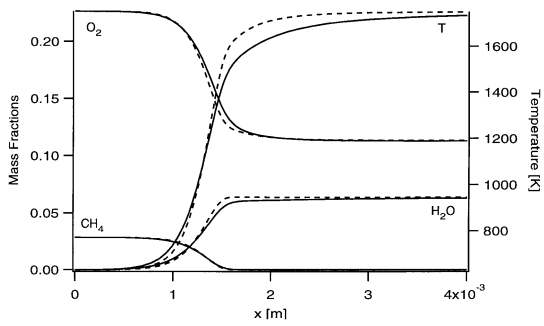

Fig. 6. Temperature and main species profiles of laminar flames computed with the base (—) and the optimized two-step (– – –) mechanism with rate coefficient set 2/qc2/p1 (see Table 1) as principal rates.

As we are interested in applications to gas turbine combustion, it is necessary to validate the rate coefficient optimization procedure also at elevated pressures. We have chosen $p = 20$ bar, $T_o = 753$ K, and again $\phi = 0.5$ as a test case representative of a modern gas turbine. As in the atmospheric case, a freely propagating premixed laminar flame at these conditions computed with the Miller-Bowman mechanism [20] served both to provide detailed concentration and rate data for the optimization and to validate computations using the simplified mechanism (13) with optimized rate coefficients. The representability analysis suggests that $\{\dot{q},\ \dot{\omega}_{CO_2}\}$ or $\{\dot{\omega}_{H_2O},\ \dot{\omega}_{CO_2}\}$ should be chosen as principal rates; with $\{\dot{\omega}_{CH_4},\ \dot{\omega}_{CO_2}\}$ heat release rates and production of H_2O and CO are too large at lower temperatures, while as already observed at $p = 1$ bar, $\{\dot{q},\ \dot{\omega}_{CO}\}$ results in a rate curve that seems incompatible with the Arrhenius ansatz.

The optimization procedure converged again without problems, provided that sufficiently high activation energies of order $E_A/R \sim 30{,}000$ K are present in the initial population. With such high activation energies (see also Table 1), excellent agreement between the base mechanism's principal rates and the optimized two-step mechanism has been achieved; see Fig. 8. Note that at $p = 20$ bar, a local minimum of $\tilde{r}_1$, as observed at atmospheric pressure around approximately 90% reaction progress, is no longer present. With $\dot{\omega}_{H_2O}$ instead of $\dot{q}$ as the

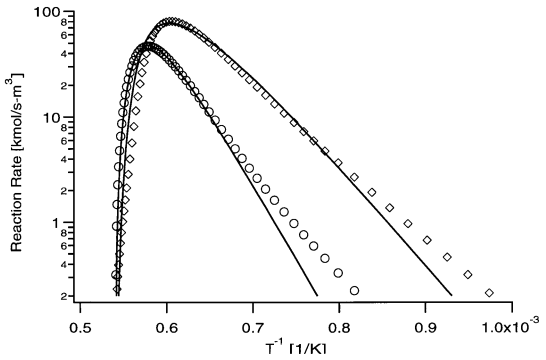

Fig. 8. Comparison of optimized rates (—) for the two-step mechanism (13) with rate coefficients 2/qc2/p20 and principal rates $\dot{q}$ (◇) and $\dot{\omega}_{CO_2}$ (○) of the base mechanism (detailed concentration and rate data taken from a freely propagating flame computation at $p = 20$ bar, $T_o = 753$ K, and $\phi = 0.5$).

first principal rate, an almost identical plot is obtained (not shown). The profiles of temperature and main species (see Fig. 9) also show how accurately the optimized mechanism matches the flame structure obtained with the base mechanism. The flame speed $S_L = 0.229$ m/s obtained with detailed chemistry has also been reproduced by the two-step chemistry: $S_L = 0.233$ m/s for $\tilde{\mathbf{p}} = \{\dot{q}, \dot{\omega}_{CO_2}\}$ and $S_L = 0.235$ m/s for $\tilde{\mathbf{p}} = \{\dot{\omega}_{H_2O}, \dot{\omega}_{CO_2}\}$. Only CO burn-out is not entirely satisfactory for our purposes, as carbon monoxide mass fractions approach the equilibrium level of $Y_{CO} = 1.3 \times 10^{-5}$ too slowly, especially so with $\tilde{\mathbf{p}} = \{\dot{q}, \dot{\omega}_{CO_2}\}$; see Fig. 10.

The improved agreement of simplified and base mechanisms at elevated pressure can be explained by the lower levels of intermediate

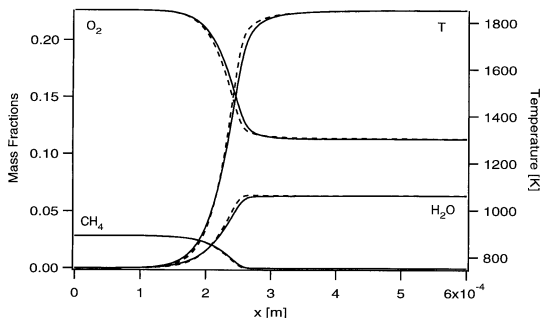

Fig. 9. Temperature and main species profiles of a laminar flame at elevated pressure computed with the base (—) and an optimized two-step mechanism with rate coefficients 2/qc2/p20 (– – –).

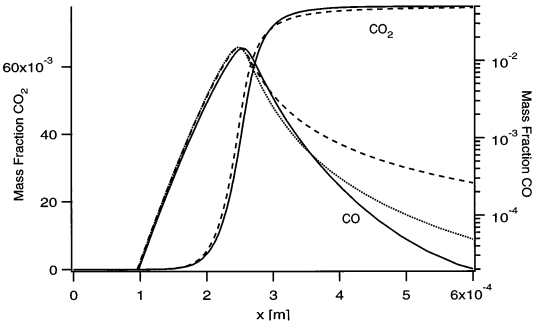

Fig. 10. CO_2 and CO profiles of a laminar flame at pressure $p = 20$ bar computed with the base (—) and optimized two-step mechanisms with rate coefficients 2/qc2/p20 (– – –) and 2/hc2/p20 (· · ·).

species within the flame's reaction zone, which results in a better match of the temperature profile above 1600 K.

THREE-STEP MECHANISM

The prediction of NO_x emissions from a lean-premixed combustor hinges on the correct prediction of O, OH, and H radical concentrations, all of which are of fundamental importance for NO_x formation via the Zeldovich and the nitrous oxide path; see, e.g., [24]. Although it has been shown [7, 25] that O-atom levels (as well as NO formation rates) may be correlated with CO concentrations in lean-premixed combustion, it seems desirable to explore approaches which more directly exploit knowledge about detailed chemical kinetics in the prediction of oxyhydrogen radical concentrations.

If H_2 is part of a simplified mechanism, the assumption of partial equilibrium in the oxyhydrogen radical pool allows the determination of the corresponding radical concentrations from oxygen and hydrogen concentrations and temperature. A three-step mechanism with CO and H_2 as intermediates has been derived by Peters and Williams [1] with the systematic reduction technique:

$$\begin{aligned} CH_4 + O_2 &\rightarrow CO + H_2 + H_2O, \\ CO + H_2O &\rightarrow CO_2 + H_2, \\ 2H_2 + O_2 &\rightarrow 2H_2O. \end{aligned} \tag{17}$$

Rather than using the rate expressions supplied by the systematic reduction technique, we use

again the genetic algorithm to determine the coefficients of rate expressions in Arrhenius form. Note that in this first application of our method to a three-step mechanism, no reverse reactions are considered.

From our experience with the two-step mechanism, the combination $\tilde{\mathbf{p}} = \{\dot{q}, \dot{\omega}_{H_2O}, \dot{\omega}_{CO_2}\}$ of heat release and products creation rates would seem to be a natural choice for the principal rates. In this case, the principal system matrix $\tilde{\mathcal{M}}$ and its inverse are

$$\tilde{\mathcal{M}} = \begin{pmatrix} -h_1 & -h_2 & -h_3 \\ 1 & -1 & 2 \\ 0 & 1 & 0 \end{pmatrix}, \tag{18}$$

$$\tilde{\mathcal{M}}^{-1} = \frac{1}{h_3 - 2h_1} \begin{pmatrix} 2 & h_3 & h_3 + 2h_2 \\ 0 & 0 & h_3 - 2h_1 \\ -1 & -h_1 & -h_1 - h_2 \end{pmatrix}. \tag{19}$$

However, this set of principal rates shows extremely poor reproducibility of the base mechanism's rates with the three-step mechanism, both at atmospheric and high pressure. In particular, the reaction rates r_1 and r_3 display large negative peaks around $T \approx 1550$ K and $T \approx 1200$ K, respectively.[4] Furthermore, the minor rates are very poorly reproduced by the three-step mechanism with this choice of principal rates (not shown).

Fortunately, choosing other combinations of rates, e.g., $\tilde{\mathbf{p}} = \{\dot{\omega}_{CH_4}, \dot{\omega}_{H_2O}, \dot{\omega}_{CO_2}\}$ or $\tilde{\mathbf{p}} = \{\dot{q}, \dot{\omega}_{H_2}, \dot{\omega}_{CO_2}\}$ yields excellent representability and rate distributions that are compatible with the Arrhenius ansatz. Finding optimized rate coefficients (see Table 1) for these two sets of principal rates proved to be no difficulty. Again the activation energies at $p = 20$ bar are significantly higher than at atmospheric pressure. Computed flame speeds at atmospheric pressure are $S_L = 0.470$ m/s for the rate coefficient set 3/fw2/p1 (see Table 1) and $S_L = 0.490$ m/s for 3/qh2/p1, agreeing very well with the value $S_L = 0.482$ m/s obtained with the base mechanism. At $p = 20$ bar, where the laminar flame speed obtained with the base mechanism equals 0.229 m/s, the agreement is also excellent: $S_L = 0.230$ m/s for rate coefficient set 3/qh2/p20 and $S_L = 0.225$ m/s for set 3/fw2/p20 (see Table 2).

[4] Upon inspection of the rate distributions, it is easy to see how the negative rates come about: $h_2 \ll h_1, h_3$ for the mechanism (18), and therefore $\tilde{r}_1 \propto 2\dot{q} + h_3(\dot{\omega}_{CO_2} + \dot{\omega}_{H_2O})$ with good accuracy. It turns out that the two terms in this sum are of nearly equal magnitude but of opposite sign.

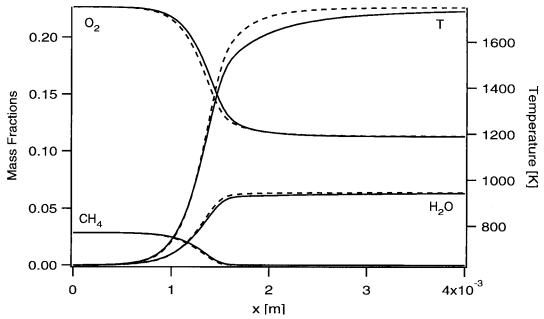

Fig. 11. Temperature and main species profiles of a laminar flame at atmospheric pressure computed with the base (—) and an optimized three-step (– – –) mechanism with $\{\dot{\omega}_{CH_4}, \dot{\omega}_{H_2O}, \dot{\omega}_{CO_2}\}$ as principal rates (rate coefficient set 3/fw2/p1).

Plotting main species and temperature profiles obtained with the base and the three-step mechanism, respectively, yields graphs that are very similar to Figs. 6 and 9 if the x-axis scale is adjusted for the reduced flame thickness, which is an order of magnitude smaller in the high pressure case. Discernible differences are found only for H_2O, where the three-step mechanism yields slightly better agreement with detailed chemistry results (see Fig. 11). Peak levels of CO and H_2 are well reproduced for both pressure cases; however, as already observed with the two-step mechanism, for both intermediate species the return to equilibrium is too fast. Profiles of CO and H_2 for the atmospheric case are shown in Fig. 12. At $p = 20$ bar, the peak value of H_2 mass fraction is with approximately 8×10^{-5} much smaller; other than that the results for the intermediates are equivalent to the atmospheric case.

OFF-DESIGN APPLICATIONS OF OPTIMIZED MECHANISMS

As already mentioned in the Introduction, the goal of our rate coefficient optimization is not to determine one set of rate coefficients applicable to a wide range of operating conditions. Indeed, we surmise that it is not possible to find rate coefficients for two- or three-step mechanism as

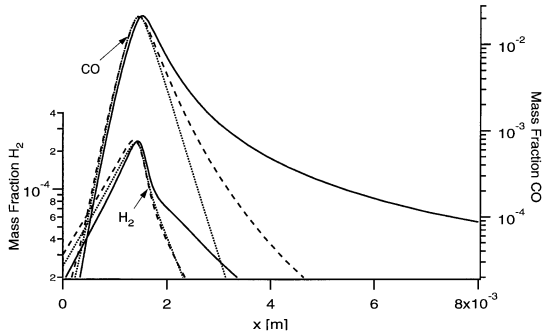

Fig. 12. CO_2 and H_2 profiles of laminar flames at atmospheric pressure computed with the base (—) and optimized three-step mechanisms with rate coefficient sets 3/fw2/p1 (– – –) and 3/qh2/p1 (· · ·). At equilibrium, $Y_{CO} \approx 1.7 \times 10^{-5}$, while $Y_{H_2} \approx 6.9 \times 10^{-7}$.

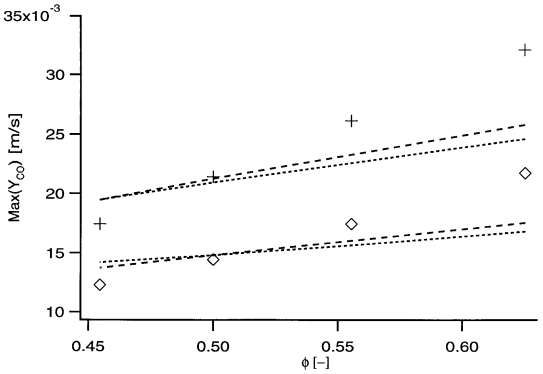

Fig. 14. Maximum CO mass fraction in laminar flames computed with a detailed mechanism at $p = 1$ bar (+) and $p = 20$ bar (◇) and with two-step (· · ·) and three-step (– – –) mechanisms.

they are used in this work, that reproduce, e.g., flame speed and structure of both fuel-rich and -lean flames. Nevertheless, we do expect that any given set of coefficients should be reasonably accurate in the vicinity of its "design point," i.e., the operating conditions of the laminar flame computation with the base mechanism that provides concentration and rate information for the representability analysis and the genetic algorithm. In other words, we expect that the region in the space of thermodynamical state variables where a given set of optimized rate expressions may be used is somewhat larger than the region spanned by the data set used to determine the rate coefficients.

As a first example of an off-design application of simplified mechanisms, we summarize in Figs. 13 and 14 laminar flame speeds and CO peak mass fraction of premixed laminar flames at equivalence ratios $\phi = 0.625$, 0.55, 0.5, and 0.454, at both $p = 1$ bar and $p = 20$ bar. Here the design point is $\phi = 0.5$, predictions of both two-step and three-step mechanisms with rate coefficient sets 2/qc2/p1, 2/qc2/p20, 3/fw2/p1, and 3/fw2/p20 are compared against those of the base mechanism of Miller and Bowman [20]. Concerning flame speeds, the agreement between the detailed and the simplified mechanisms is very impressive over the whole range of equivalence ratios ϕ covered. Also profiles of temperature and main species computed with the simplified mechanisms agree very well with those of the computations with detailed chemistry (not shown). The increase of Y_{CO} peak levels with increasing ϕ, on the other hand, is underpredicted by the simplified mechanism (see Fig. 14). A similar observation is made concerning H_2 mass fraction (not shown).

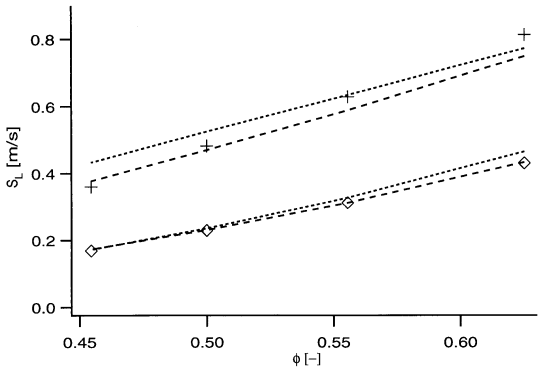

Fig. 13. Laminar flame speeds computed with a detailed mechanism at $p = 1$ bar (+) and $p = 20$ bar (◇) and with two-step (· · ·) and three-step (– – –) mechanisms.

A second example is the computation of a strained flame with a simplified mechanism based on detailed chemistry data from a freely propagating (unstrained) laminar flame. Operating conditions are in both cases $\phi = 0.5$, $T_i = 753$ K, and $p = 20$ bar. The strain rate $a = 20{,}000\ s^{-1}$ is quite high, the heat release zone has been driven by the approach flow to the stagnation point at $x = 0$, and the flame thickness has been reduced to about one half of its unstrained value (see Fig. 15). Nevertheless, both the two-step (not shown) and the three-step mechanisms match the temperature and main species profiles quite well. The distributions of the inter-

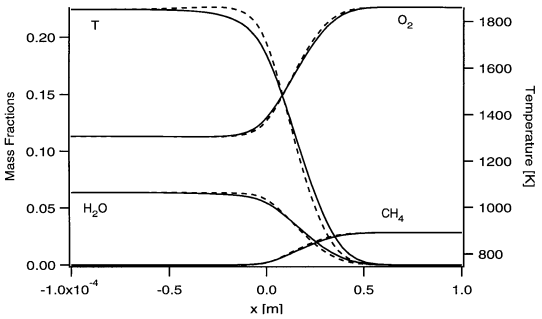

Fig. 15. Temperature and main species profiles of a strained laminar flame with $a = 20{,}000\ s^{-1}$, $\phi = 0.5$, $T_i = 753$ K, and $p = 20$ bar. Data are obtained with the base mechanism (—) and with an optimized three-step mechanism (3/fw2/p20; see Table 2). The two-step mechanisms produce nearly identical results, only the slight temperature overshoot, caused presumably by preferential diffusion of H_2, is absent.

mediates CO and H_2 are also well reproduced by the simplified mechanisms; see Fig. 16.

Phenomena of great importance to the gas turbine design work are, among others, fuel-air inhomogeneities, heat losses, and film cooling air admixing. The demonstrated possibility to extrapolate from the design point makes our approach particularly suitable for the investigation of these phenomena with turbulent combustion models. Also, the use of kinetic data from an unstrained laminar flame as basis for the coefficient optimization should not restrict the use of the coefficients to the flamelet regime of turbulent combustion. In comparison, methods using lookup-tables or flamelet libraries are unavoidably restricted to that region in the space of thermodynamical state variables where the tables or libraries were generated. This would necessitate the use of data sets of high dimension and very large size in the applications that we envisage, leading to very high costs for generation, storage, and retrieval of rate data.

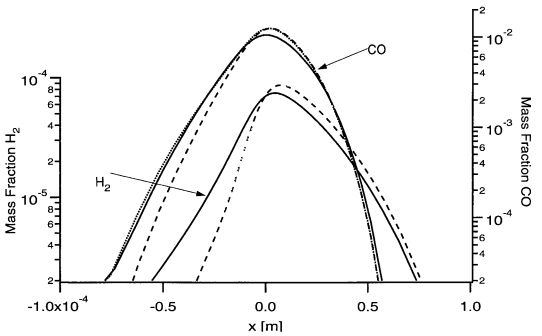

Fig. 16. CO and H_2 profiles of a strained laminar flame with $a = 20{,}000\ s^{-1}$, $\phi = 0.5$, $T_i = 753$ K, and $p = 20$ bar. Data are obtained with the base mechanism (—) and with optimized two-step ($\cdots$) and three-step (– – –) mechanism (2/hc2/p20 and 3/fw2/p20, respectively; see Table 2).

SUMMARY AND CONCLUSIONS

It has been demonstrated that two- or three-step mechanisms with optimized rate coefficients describe many of the important features of lean-premixed methane combustion with good accuracy. This is particularly so at elevated pressure, where concentrations of intermediates that are absent in the simplified mechanism are much lower than at atmospheric conditions.

The objective of this work was not to determine one set of rate coefficients for methane combustion that is valid for a wide range of temperatures, pressures, or equivalence ratios. Instead, we have tried to develop a method, applicable to gaseous fuels for which a detailed mechanism is available, that allows to quickly find rate coefficients for particular operating conditions by matching heat release and species production rates of the simplified mechanism to those of an underlying detailed chemical mechanism. A genetic algorithm has been employed to carry out the matching, i.e., determine rate coefficient that minimize a suitably defined cost function. With this approach, minimum human effort and little insight into the details of the chemical mechanism (time scale analysis, identification of quasi-steady-state species, etc.) is required to generate sets of optimized rate coefficients.

As a pre-processing step for the genetic algorithm, it is recommended to carry out a "representability analysis." This analysis identifies so-called "principal rates" and defines a linear mapping between the principal rates and the reaction rates of the simplified mechanism. It is then easy to check to what extent rate distributions of the base mechanism can be reproduced consistently by the simplified mechanism and whether the rate data are compatible with the Arrhenius ansatz for the rate law. Also, the linear mapping reformulates the problem of matching heat release or species production

rates as a problem of matching reaction rates. This makes it possible to apply a divide and conquer strategy to the optimization problem, which brings about, even for the relatively simple two- or three-step mechanisms discussed in this work, a significantly improved convergence behavior for the optimization algorithm.

The most significant deficiency of our approach that has been identified so far concerns the prediction of CO or H_2 burn-out, which does not match the base mechanism's behavior. However, it is expected that the introduction of reverse reactions combined with a suitable redefinition of the cost function or the rate-law ansatz will bring improvement in this respect.

In conjunction with a turbulent combustion model suitable for modeling lean-premixed turbulent combustion in, e.g., gas turbines, simplified mechanisms with optimized rate constants should allow to investigate the impact of design changes on phenomena such as temperature distributions, extinction limits, NO_x production and, provided that the shortcomings mentioned in the previous paragraph can be overcome, CO burn-out. Our experience with "off-design" applications of sets of optimized rate coefficients suggests that this is so even in circumstances where equivalence ratio or enthalpy are not constant throughout the combustor. For many engineering applications, simplified mechanisms with optimized rate coefficients might due to their simplicity, flexibility, efficiency, and robustness be an attractive alternative to competing strategies for simplifying chemical kinetics [1–6], although the latter methods are perhaps conceptually more appealing, as they rest on a more fundamental analysis of the underlying detailed chemical kinetics.

We are indebted to Hans Jürg Wiesmann and Jakob Bernasconi for inspiring discussions on traditional optimization schemes and on the problem of representability. We are grateful to Bernhard Rogg and Weigang Wang for making the RUN-1DL program available, and to Robert Kee and Fran Rupley for providing the CHEMKIN-II software.

REFERENCES

1. Peters, N., and Williams, F. A., *Combust. Flame* 68: 185–207 (1987).
2. Smooke, M. D., Editor, *Reduced Kinetic Mechanismus and Asymptotic Approximations for Methane-Air Flames*, Springer-Verlag, Berlin (1991).
3. Peters, N., and Rogg, B., Editors, *Reduced Kinetic Mechanisms for Applications in Combustion Systems*, Springer-Verlag, Berlin (1993).
4. Lam, S. L., *Combust. Sci. and Tech*. 89:375–404 (1993).
5. Maas, U., and Pope, S. B., *Combust. Flame* 88:239–264 (1992).
6. Polifke, W., Döbbeling, K., Sattelmayer, Th., Nicol, D. G., and Malte, P. C., *Transactions of the ASME. J. Eng. for Gas Turbines and Power* 118:765–772 (1996).
7. Nastoll, W., *Private communication* (1992).
8. Coffee, T. P., Kotler, A. J., and Miller, M. S., *Combust. Flame* 54:155–169 (1983).
9. Jiang, B., Ingram, D., Causon, D., and Saunders, R. *Shock Waves* 5:81–88 (1995).
10. Nicol, D. G., Dissertation, Univ. of Washington (1995).
11. Abdalla, A. Y., Bradley, D., Chin, S. B., and Lam, C., *Oxidation Communications* 4:113–130 (1983).
12. Westbrook, C. K., and Dryer, F. *Combust. Sci. Tech*. 27:31–43 (1981).
13. Coffee, T. P., *Combust. Sci. Tech*. 43:333–339 (1985).
14. Lolos, P., "Untersuchung der Struktur von mageren Vormischflammen und deren Einfluss auf die NOx Bildung." Diplomarbeit, RWTH Aachen (1995).
15. Jones, W. P., and Lindstedt, R. P., *Combust. Flame* 73:233–249 (1988).
16. Frouzakis, C. E., Private communication (1996).
17. Roekarts, D. and van der Meer, Th., Abstracts of the EUROMECH Colloquium 340, "Statistical Properties of Turbulent Gaseous Flames" (1995).
18. Rogg, B., Technical Report CUED/A-THERMO/TR39, University of Cambridge, Dept. of Engineering, (1991).
19. Rogg, B., "RUN-1DL; The Cambridge Universal Laminar Flamelet Computer Code." In N. Peters and B. Rogg, Ed. *Reduced Kinetic Mechanisms for Applications in Combustion Systems*. Springer Verlag (1993).
20. Miller, J. D., and Bowman, C. T., *Prog. Energ. Combust. Sci*. 15:287–338 (1989).
21. Kee, R. J., Rupley, F. M., and Miller, J. A., Sandia Report SAND89-8009B UC-706, (1989).
22. Rechenberg, I.: *Evolutionsstrategie '94*, Frommann-Holzboog, Stuttgart-Bad Cannstadt (1994).
23. Press, W. H., Flannery, B. P., Teukolsky, S. A., and Vetterling, W. T.: *Numerical Recipes*, Cambridge University Press, Cambridge, (1989).
24. Nicol, D. G., Steele, R. C., Marinov, N. M., and Malte, P. C., *Transactions of the ASME, Journal of Engineering for Gas Turbines and Power*. 117:100 (1995).
25. Nicol, D. G., Malte, P. C., and Steele, R. C., Paper 94-GT-432, ASME, New York (1994) to appear in *Transactions of the ASME*.

Received 10 January 1997; accepted 11 June 1997